On the structure and photoluminescence of dislocations in silicon

L. I. Fedina,[a)] A. K. Gutakovskii, and T. S. Shamirzaev

Rzhanov Institute of Semiconductor Physics, Novosibirsk 630090, Russia

This paper presents a comparative analysis of the structure and photoluminescence (PL) of Si containing dislocations introduced by thermal shock or ion implantation. To study the structure of dislocation cores and their interaction with point defects, we used a high-resolution transmission mode during *in situ* electron irradiation in the JEM4000EX operating at 400 kV. An appropriate PL spectrum was obtained on dislocated Si after electron irradiation by an external pulse gun operating at 350 kV. This resulted only in an increase in the D2 line intensity that correlated with the formation of metastable interstitial defects on {001}, {111}, and {113} planes near various dislocation cores during *in situ* electron irradiation, regardless of their types. However, the D1 line relates to a core structure of a shuffle Lomer dislocation consisting of 5/7 atomic rings, which occurs when two shuffle 60° dislocations (so-called S1 type [Pizzagalli *et al.*, Phys. Rev. Lett. **103**, 065505 (2009)]) combine with each other in intersecting {111} planes in plastically deformed Si or when an extrinsic Frank partial dislocation transforms into a perfect one in an ion-implanted layer. *Published by AIP Publishing.* https://doi.org/10.1063/1.5011329

I. INTRODUCTION

Electronic properties of dislocations and dislocation-related luminescence (DRL) in Si have been studied for many years (see, for example, review[1]). However, despite the vast amount of work done in the last three decades, some aspects of DRL are far from being totally understood. Major concerns arise from the unknown nature of optically active centers related to D1 and D2 lines and from the elusive role played by impurities and point defects in their appearance. In general, the observation of D1/D2 lines does not depend on the method used for introducing dislocations.[2–9] It is assumed that they are related to dislocation jogs[3,10] and intersections,[4] impurity and point defect clusters trapped in a core,[11,12] and dislocation segments of special types [such as Lomer dislocations (LDs)] appearing as a result of dislocation reactions.[1] However, because of the large variety of types of dislocations involved in DRL, it is difficult to single out one that may be responsible for D1/D2 lines.

Dislocations in diamond structure Si can assume two sets of configurations, i.e., the shuffle set and the glide set, depending on whether their cores are located on widely or narrowly spaced {111} planes.[13] A reliable correlation between the D3/D4 lines and the dissociated 60° dislocations located on the glide set of {111} planes was previously established.[3,14] Recently, it is found that shuffle dislocations introduced under gigapascal stresses are optically inactive.[15] These dislocations are known to be undissociating,[16] but their subsequent annealing at temperatures above 400 °C leads to an appearance of all D1-D4 lines.[17] This strongly suggests that annealing causes changes in dislocation configurations.[18] It is obvious that a further way for probing the nature of DRL should include a search of reliable correlations between dislocation core transformations and changes in their optical activity. The solution to this problem requires the use of *in situ* methods that make it possible to observe core transformations in real time, for instance, during electron irradiation in a high-resolution transmission electron microscope (HRTEM).[19]

Many models of dislocation core structures, necessary for the understanding of DRL in Si, were earlier proposed by Hornstra,[20] including glissile dissociated and undissociated 60°, and two types of sessile 90° dislocations. The latter are often called pure edge or Lomer dislocations (LDs),[21] assuming that their cores have Hornstra-like shuffle or glide structures. The core of a shuffle LD consists of closely bonded five- and seven-membered (5/7) atomic rings, whereas a single eight-membered ring having an atom with two dangling bonds characterizes a glide LD core.[22,23]

State of the art theoretical[24] and experimental[25–30] studies not only confirmed Hornstra's models, but also discovered new properties of an undissociated 60° dislocation. According to first-principles calculations, there are four core configurations of this dislocation: S1, S2, S3 of the shuffle set, and G of the glide set.[24] Only one of them, the S1, is mobile, while the other three are sessile. The main difference between mobile and sessile cores is the presence of a dangling bond in the S1 core that inevitably implies the loss of its optical activity.[31] The necessary transformation of the S1 core to the "glide" G type being able further to dissociate requires the S1 to climb to the glide set of {111} planes.[16] As mentioned above, the dissociation[32] leads to the appearance of D3/D4 lines. Therefore, D1/D2 lines could be related to the undissociated G type core. In addition, two mobile S1 dislocations can combine in intersecting {111} planes to form the shuffle LD core without any dangling bonds. Both "glide" G and shuffle LD cores consist of 5/7 atomic rings[22–24,33] and, therefore, may contribute similarly to the D1/D2 lines. Large-scale *ab initio* calculations[34] show that the 5/7-LD core brings a deep level (~0.2 eV) to the fundamental gap of

a)E-mail: fedina@isp.nsc.ru

Si, which may provide an appearance of the D1 line. However, nothing is known about the electronic states related to the "glide" G dislocation. Moreover, unlike the S1 and various LD cores, whose structures have already been determined by means of high-resolution transmission (HRTEM)[22,23] and aberration-free electron microscopy,[25–30] the structure of the G core still has not been visualized.

In this paper, based on the fundamental knowledge accumulated to date and the results obtained here using *in situ* HRTEM irradiation supported by a structural modeling, image simulations, and the geometrical phase analysis (GPA) we will discuss the influence of dislocation core structures and their interaction with point defects on DRL, in particular, on the appearance of D1/D2 lines.

II. EXPERIMENTAL PART

Extrinsic Frank partial and perfect prismatic dislocation loops were obtained in CZ-Si wafers by Si^+, B^+, and O^+ ion implantation with 30–150 keV energy and doses of 4×10^{14} or 10^{16} cm^{-2} followed by annealing at T = 900–1000 °C. Sliding dislocations in Fz-Si were introduced by thermal shock, when the growth process of Si ingots ceased due to a spillage of the molten zone. The interaction of point defects with dislocation cores was studied during *in situ* electron irradiation in the JEM4000EX operating at 400 kV at room temperature. The flux of electrons on a specimen during irradiation in the microscope was estimated to be about 10^{20} cm^{-2} s^{-1}. Additionally, a surface area ($\sim$1 cm^{-2}) of dislocated FZ-Si specimen was irradiated by an external electron gun with 350 kV to a dose $\sim$10^{20} cm^{-2} to measure a photoluminescence (PL) spectrum in appropriate conditions. Models of dislocation cores necessary for simulation of HRTEM images were constructed within the $102 \times 102 \times 112$ Å supercell (27 000 atoms) of Si and were optimized by Mm+ force field calculations (HyperChem-8.0). For image simulations, we used a multislice program MUSLI.[35] PL was excited by an Ar$^+$ laser ($\lambda = 488$ nm) and detected at a temperature of 4.2 K by a liquid nitrogen-cooled Ge p-i-n photodiode EI-L.

III. RESULTS AND DISCUSSION

A. The structure and PL of sliding 60° dislocations

Figure 1 shows the distribution of dislocations in Fz-Si (a) and their TEM analysis (b)–(d). According to selective etching data, the dislocation density varies locally from $\sim$10^6 to $\sim$10^7 cm^{-2} and dislocation trails are located in intersecting {111} planes [Fig. 1(a)]. TEM and weak beam [Figs. 1(b)–1(d)] images displace nanopores, which are the source of these undissociated dislocations. Figure 2 presents [110] HRTEM images of these dislocations at the initial (a) and short-time (b), (c) stages of *in situ* electron irradiation. A model of dislocation core corresponding to the initial stage of irradiation and its simulated image are shown in (a) as left and right insets, respectively. The Burgers contour drawn around the dislocation indicates that its vector $\boldsymbol{b} = $ a/2 $\langle 110 \rangle$ lies on the {111} plane and corresponds to an undissociated 60° dislocation. Its core structure obtained by Mm+
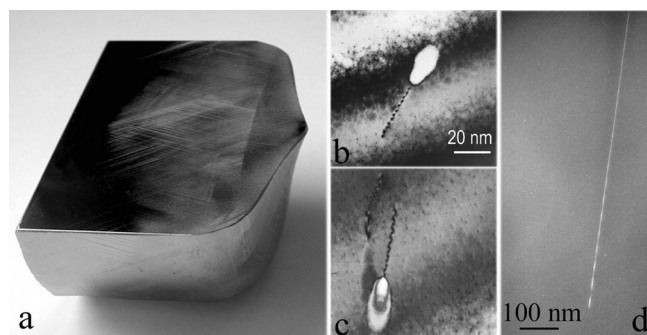

FIG. 1. Optical image (a) of dislocations in (110) cross-section of an FZ-Si ingot after selective etching and their TEM (b), (c) and weak beam (d) images.

optimization [Fig. 2(a), left inset] is similar to the one proposed by Hornstra[20] and calculated from first principles (as-called S1 type).[24] One can see that the core consists of a single eight-membered atomic ring having one atom carrying a dangling bond marked by (*) in the model. A good agreement between the experimental [Fig. 2(a)] and simulated images [Fig. 2(a), right inset] supports the observation of the shuffle S1 core. One more proof is presented in Fig. 3 which shows enlarged experimental (a), (b) and simulated (c) HRTEM images of an (001) defect observed near a dislocation core in Fig. 2(b). While the structure of this defect does not reach its equilibrium state during the short duration of electron irradiation, the simulated image fits well with the experimental one. Note, that for the image simulation we used an optimized model (not shown) of the (001) defect structure experimentally observed in Fig. 3(b). This defect consists of (2×1) an ordered sequence of single eight- and double-five atomic rings located on the (001) plane. Each pair of the five-membered rings is created by four self-interstitial atoms (I_4 cluster), one of which is attached to the core. One can see that the core keeps an atom carrying a dangling bond after the attachment of I_4 cluster [Fig. 3(b)]. This confirms the observation of the S1 core.

A single I_4 cluster placed inside a core of 90° partial was proposed by *ab initio* calculations to be responsible for the D1/D2 lines.[36] However, Fig. 3(b) demonstrates that the I_4 cluster is attached outside the S1 core, in its tensile part, to ensure the core relaxation. According to molecular dynamic simulations, the {001} defects can be found in both zero pressure and tensile strained simulations.[37]

Now let us return to the results concerning the involvement in DRL of interstitial defects introduced near cores by electron irradiation, as represented in Figs. 2(b)–2(d). It is seen that all D1-D4 lines are observed in PL spectra of dislocated Fz-Si and only the intensity of the D2 line increases substantially after electron irradiation by an external pulse gun [Fig. 2(d), line 2]. At the same time, HRTEM images show that dislocation cores effectively interact with self-interstitials (*Is*) generated by electron irradiation in the microscope [Figs. 2(b) and 2(c)]. As a result, all known types of metastable interstitial defects located on {111}, {113}, and {001} habit planes[19,38,39] arise near cores. These defects can be formed independently of the presence of dislocations in Si up to $T \sim 0.5T_m$, where T_m is the melting point of Si.[38]
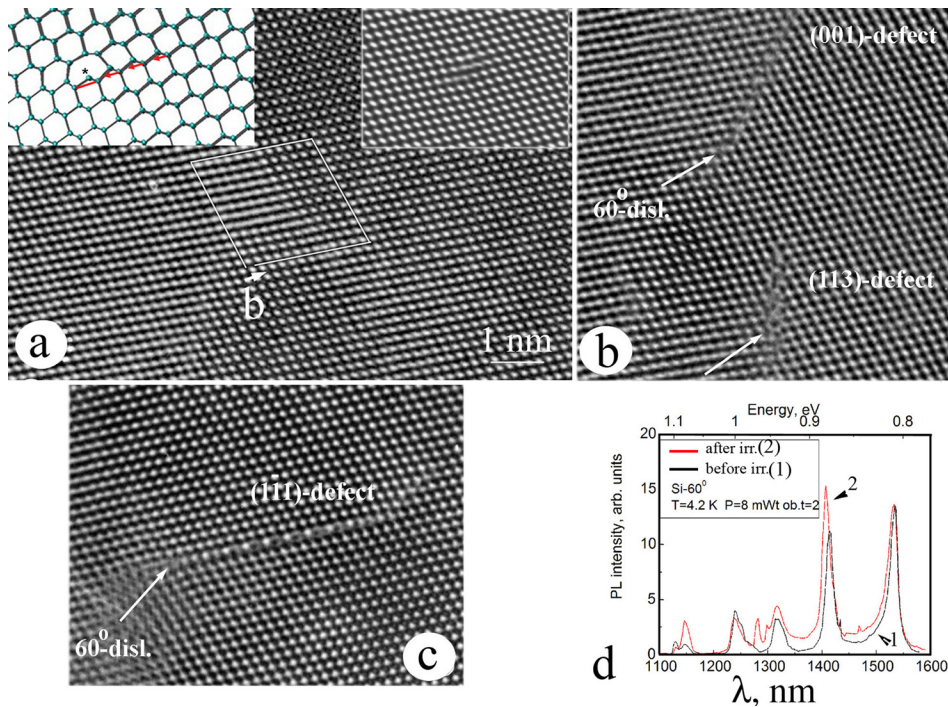
FIG. 2. [110] HRTEM images of dislocations in Fz-Si before (a) and after ~1–2 min of *in situ* electron irradiation in JEM-4000EX at room temperature (b), (c). Insets in (a) are a model of S1 dislocation (left) and its simulated image (right). Red line and arrows in the model show S1-G core transformations followed by Shockley partial gliding after the emission of an atom (*) from the S1 core. Parameters of image simulation: thickness of crystal 6.1 nm, defocus value (−45) nm. White arrows in (b), (c) show cores of dislocations. (d) PL spectra of dislocated Fz-Si before (black line 1) and after (red line 2) electron irradiation by external pulse gun.

Because of high (~1.3 eV) energy barrier for *Is* embedding into lattice sites leading to a climb of dislocations,[40] they can be accumulated near cores only as metastable defects, ensuring a core relaxation.[19] Thus, dislocation cores at $T < 0.5T_m$ simply act as nucleation centers of metastable defects. We will not discuss here the formation of {111} and {113} defects near cores; their expanded descriptions can be found elsewhere.[19,41,42]

Note that the dose of electrons supplied by an external pulse gun was about two orders of magnitude less than that in the electron microscope. It is clear that the defects of smaller sizes but of similar features provoke the D2 line appearance in PL spectrum [Fig. 2(d)]. Apart from the increasing intensity of the D2 line related to interstitial defects near dislocation cores, a small additional PL peak between D3 and D4 bands appears after irradiation by an external electron gun [Fig. 2(d)]. This PL probably originates from very small *Is* clusters not bonded to dislocation cores, which are known to induce the proper PL line at 0.97 eV (1.28 μm).[43]

As concerns about the D1 line in PL spectra of Fz-Si [Fig. 2(d)], where the S1 dislocations slide in intersecting {111} planes [Fig. 1(a)], we assume that in this case the formation of shuffle LDs is inevitable and, as discussed above, it may lead to the appearance of this line. Unfortunately, the dislocation density in Fz-Si was too small to observe LDs by TEM. However, we are sure that they are detected in PL spectra over a much larger area compared with TEM.

B. The structure and PL of dislocations in ion-implanted Si

The formation of extrinsic Frank partial and perfect prismatic dislocation loops in ion-implanted Si has been widely studied.[38] Both dislocations are known to be sessile and of the edge 90° and 60° types, respectively. They arise due to *Is* clustering at high temperatures when *Is* integration into lattice positions is realized.[40] The DRL in ion-implanted Si has been found to be dominated by perfect dislocations.[6]

Figure 4 shows dark field TEM (a) and HRTEM (b) images of faulted Frank loops introduced in Si by a low dose $(4 \times 10^{14}$ cm$^{-2})$ self-ion implantation followed by annealing at T = 1000 °C. No other dislocations are observed in this specimen. Observation of an initial core structure in Si by using a JEM4000EX operated at 400 kV is always problematic because of the strong generation of point defects. Just
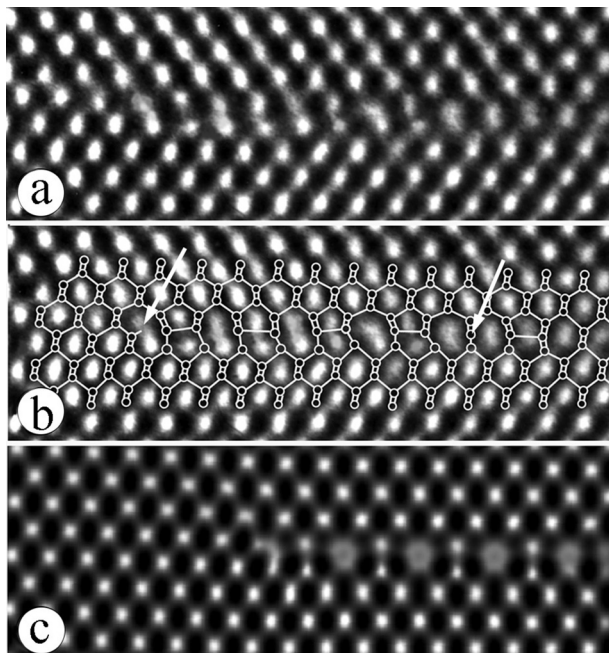

FIG. 3. [110] experimental (a), (b) and simulated (c) HRTEM images of the (001) defect attached to the S1 core, with a model superposed on the image (b). Parameters of simulations: defocus value (−40) nm, crystal thickness 6.2 nm. Left and right arrows in (b) show dangling bonds in the S1 core and within (001) defect, respectively.
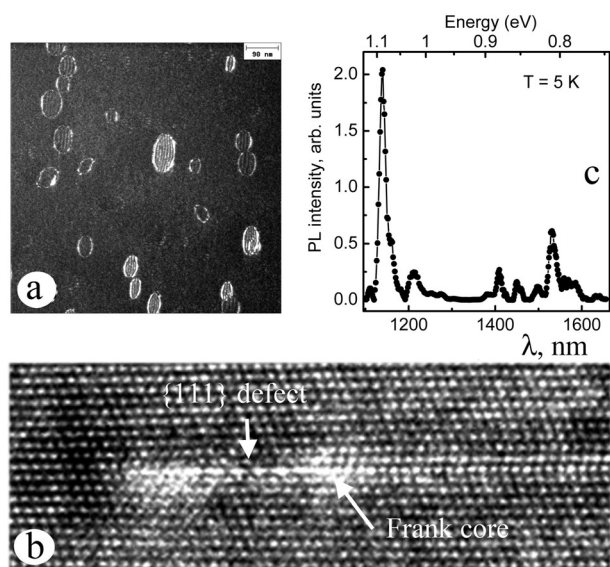
FIG. 4. TEM (a) and [110]-HRTEM (b) images of Frank partial dislocation loops introduced in Si by self-ion implantation followed by annealing at 1000 °C. (c) PL spectrum of this specimen.

after ∼1 min of irradiation a {111} defect forms close to the Frank core [Fig. 4(b)] in a similar manner to that observed near the S1 cores [Figs. 2(b) and 2(c)]. More details on {111} defect formation near both extrinsic and intrinsic Frank partial dislocations leading to the relaxation of their cores can be found in Ref. 19. The PL spectrum of Frank dislocations exhibits a very low intensity of the D1/D2 lines that suggests their weak optical activity [Fig. 5(c)].

In Si implanted with O^+ ions at a much higher dose (1×10^{16} cm^{-2}) followed by annealing at T = 900–1000 °C a mixture of faulted Frank and perfect dislocation loops, as well as long dislocation dipoles, is observed [Figs. 5(a) and 5(b)]. Note that while perfect loops form as a result of the unfaulting of the Frank loops, the dipoles appear as a result of the unfaulting of {113} defects at earlier annealing stages of Si implanted with such light ions as H^+, N^+, B^+, and O^+.[38]

The HRTEM image of a Frank dislocation in O^+-implanted Si annealed at 1000 °C also reveals a small {111} defect close to its core [Fig. 5(c), left inset] and an oxide precipitate on a stacking fault plane [Fig. 5(c)]. This image is obtained by using the JEM-2010FX operated at 200 kV at room temperature when point defects are not introduced in Si.[44] Therefore, this {111} defect was formed during the annealing of O^+-implanted Si.

Among various metastable defects, the {111} defect is the most stable one whose energy is ∼0.3 eV/atom (Ref. 19) and it may survive at high temperatures. The {111} defects undoubtedly contribute to the D2 line in PL spectra of ion-implanted Si [Fig. 5(e)].

TEM analysis shows that Frank dislocation loops transform to the perfect ones as annealing temperature increases. The greater the size of perfect loops, the higher PL intensity of the D1 line [Figs. 5(a), 5(b), and 5(e)] is. Furthermore, the intensity of the D1 line from a mixture of perfect loops and dipoles [Fig. 5(e), line 1] is 40 times that of pure Frank loops introduced by Si^+ ion implantation [Fig. 5(c)]. In Si that is highly implanted with B^+ ions and annealed at T = 900 °C,

where only faulted Frank loops are observed, DRL is completely absent [Fig. 5(e), line 3].

The image of a perfect dislocation in ion-implanted Si is shown in Fig. 5(d). One can see that the interaction of this dislocation with point defects produces severe distortions around it. However, from a magnified image [inset in Fig. 5(d)] it is seen that two {111} half-planes terminate in a core to form 5/7 atomic rings corresponding to the shuffle LD core. The Burgers contour drawn around the core results in b not lying in the {111} planes that proves an LD observation. To verify the formation of shuffle LD core, we have modeled the transformation of a faulted Frank dislocation into a perfect one using HyperChem-8.0 program. Implementation of the slip of two Shockley partials in an extrinsic layer of a Frank dislocation leads, indeed, to the formation of 5/7-LD core [Fig. 6(a)], as experimentally observed in Fig. 5(d). We have also checked the suitability of our model for analysis of a typical LD image observed by the plastic relaxation of $Ge_{0.5}Si_{0.5}$/Si(100) system [Fig. 6(b)]. Unlike 5/7-LD cores mostly formed at the Ge/Si(001) interface,[26] a glide LD core consisting of a single eight-membered atomic ring having an atom with two dangling bonds is observed here similar to that one presented in Refs. 23 and 27. For a comparative analysis of shuffle and glide LD cores, we used the geometrical phase analysis (GPA)[45,46] to map out the strain fields around the LD cores [Figs. 7(a) and 7(b)]. Although these cores differ from each other, the magnitude of elastic strains around them varies within 4%–5% depending on a stretched or compressed side of the cores [Figs. 7(c) and 7(d)]. Note the calculation of strain fields by GPA always requires a reference (i.e., strain-free) region in the HRTEM image; thus, the strain field is certainly relative. Because the reference area of the glide LD core includes an increased lattice parameter of $Ge_{0.5}Si_{0.5}$ layer [see Fig. 6(b)], its strain field increases also. Besides, the smaller the size of reference area, the higher strain fields calculated by GPA are. Specifically, strain fields around LD cores at the Ge/Si (001) interface are found to reach 10%.[29] Therefore, we conclude that our model describes satisfactory both the shuffle LD core in ion-implanted Si and glide LD core observed at the $Ge_{0.5}Si_{0.5}$/Si(100) interface.

From a comparison of the Frank partial and shuffle LD cores [Figs. 5(c) and 5(d)] it is seen that they both consist of 5/7 atomic rings; however, only the latter supplies the D1 line in PL spectra [Fig. 5(e)]. The main distinction between them is that two identical {111} half-planes terminate in the shuffle LD core, but different half-planes (one of them is a stacking fault) meet in the Frank core.

A loss of optical activity in the Frank dislocation has been explained by large-scale first-principles calculations.[34] A stacking fault adjacent to the Frank core is found to play a crucial role in mitigating the severity of traps by delocalizing their wave functions. The mixing of dislocation states with stacking fault states raises the trap levels of the Frank core from those of the shuffle LD core (∼0.2 eV) to the conduction and the valence band edges. A similar impact of an intrinsic stacking fault on a trap level position of 90° partial is also shown in Ref. 34.
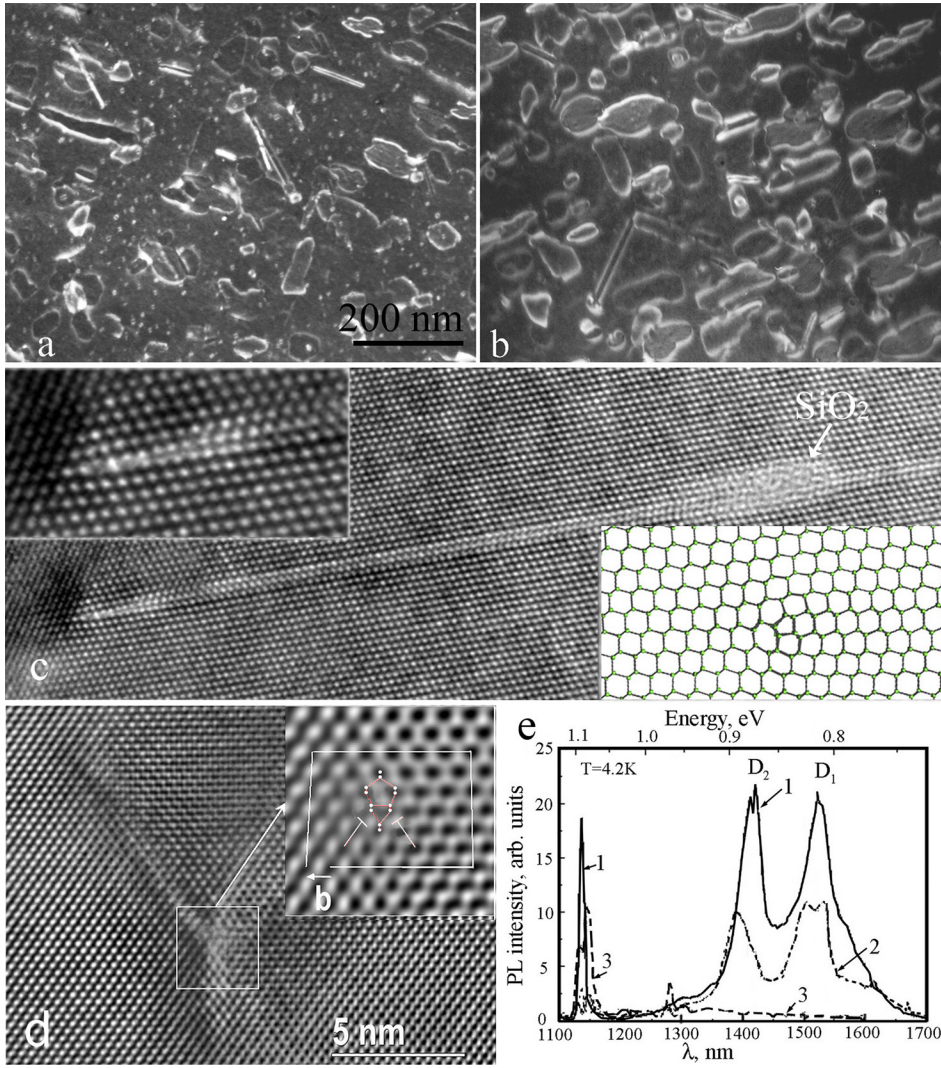
FIG. 5. TEM (a), (b) and HRTEM images of faulted Frank (c) and perfect (d) dislocations introduced by O$^+$ ion implantation followed by annealing at 900 °C (a) and 1000 °C (b)–(d). Insets in (c) are a magnified Frank core image (left) and its model. (e) PL spectra of Si implanted with O$^+$ (1, 2) and B$^+$ ions (3) implanted with a high dose (∼10^{16} cm^{-2}) and annealed at 900 °C (2, 3) or 1000 °C (1).

It is worth noting that a clear splitting of the D1 line between 0.812 and 0.830 eV takes place in oxygen-implanted Si after annealing at 900 °C [Fig. 5(e), curve 2]. This splitting is related to a high density of oxygen precipitates (∼10^{11} cm^{-2}) not bonded to dislocations [Fig. 5(a)]. A similar PL feature related to oxygen precipitates was also observed in Ref. 47.

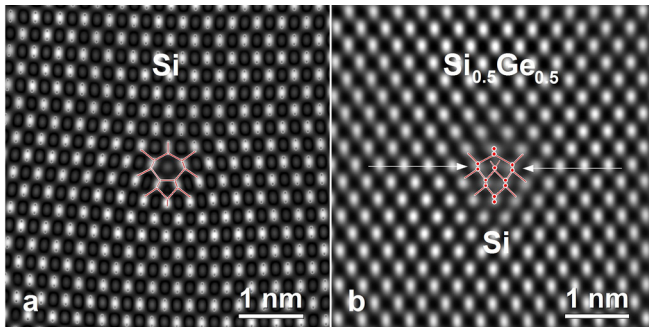FIG. 6. Simulated (with a model superimposed) (a) and experimental (b) HRTEM images of LDs in ion-implanted Si (a) and in Ge$_{0.5}$Si$_{0.5}$/Si (001) heterostructure (b). Parameters of simulation: sample thickness 25 nm, accelerating voltage 400 kV, defocus (−45) nm. The structures of shuffle and glide LD cores are traced in red lines in (a) and (b).
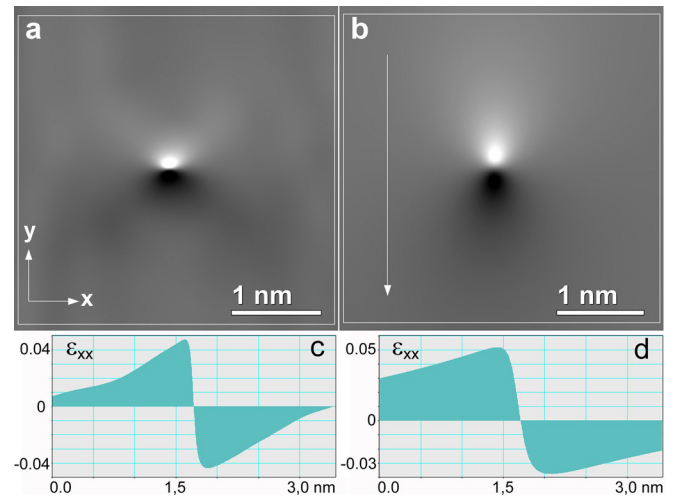

FIG. 7. The strain maps (a), (b) and the corresponding strain profiles (c), (d) for ε_{xx} near the LD cores shown in Figs. 6(a) and 6(b), respectively. The strain profiles were recorded by using the reference areas marked by white rectangles in the directions marked by the vertical arrow in (b). The GPA conditions for calculating the ε_{xx} strain map included the following selected *g*-vectors in Fourier space: 002; 00-2; 220; -2-20; 111; -1-1-1; 11-1; -1-11. The mask size: 1/4 *g* ⟨111⟩. This generalized GPA algorithm[46] makes it possible to increase the signal-to-noise ratio in phase images and the accuracy of strain measurements.

In conclusion, using both *in situ* HRTEM irradiation and *ex situ* irradiation by an external electron gun of dislocated Fz-Si, we were able to find for the first time a reliable correlation between the formation of interstitial defects near various dislocation cores and the appearance of D2 line in PL spectra. The Frank dislocations in ion-implanted Si are optically inactive, but their transformation into perfect ones accompanied with the formation of shuffle LDs leads to the D1 line emergence. This key result makes it possible to find a correlation between the D1 line and the formation of shuffle LDs in plastically deformed Fz-Si, where dominating S1 dislocations slide in intersecting {111} planes. However, depending on the transformation of interacting S1 cores, a glide LD core having two dangling bonds can also arise. This dislocation will not contribute to the DRL.

ACKNOWLEDGMENTS

[1]V. Kveder and M. Kittler, Mater. Sci. Forum **590**, 29–56 (2008).
[2]N. A. Drozdov, A. A. Patrin, and V. D. Tkachev, Sov. Phys. JETP Lett. **23**(11), 597–599 (1976).
[3]R. Sauer, J. Weber, J. Stolz, E. R. Webber, K.-H. Küsters, and H. Alexander, Appl. Phys. A **36**, 1 (1985).
[4]E. A. Steinman, V. I. Vdovin, T. G. Yugova, V. S. Avrutin, and N. F. Izyumskaya, Semicond. Sci. Technol. **14**, 582 (1999).
[5]E. Ö. Sveinbjörnsson and J. Weber, Appl. Phys. Lett. **69**, 2686 (1996).
[6]N. A. Sobolev, O. B. Gusev, E. I. Shek, V. I. Vdovin, T. G. Yugova, and A. M. Emel'yanov, Appl. Phys. Lett. **72**, 3326 (1998).
[7]X. Yu, W. Seifert, O. F. Vyvenko, M. Kittler, T. Wilhelm, and M. Reiche, Appl. Phys. Lett. **93**, 041108 (2008).
[8]Y. Yang, J. Bao, C. Wang, and M. J. Aziz, J. Appl. Phys. **107**, 123109 (2010).
[9]M. Tajima, Y. Iwata, F. Okayama, H. Toyota, H. Onodera, and T. Sekiguchi, J. Appl. Phys. **111**, 113523 (2012).
[10]G. P. Watson, J. L. Benton, Y. H. Xie, and E. A. Fitzgerald, J. Appl. Phys. **83**, 3773 (1998).
[11]V. Higgs, E. C. Lightowlers, E. A. Fitzgerald, Y.-H. Xie, and J. Silverman, J. Appl. Phys. **73**, 1952 (1993).
[12]R. Jones, B. J. Coomer, J. P. Goss, S. Öberg, and P. R. Briddon, Phys. Status Solidi B **222**, 133 (2000).
[13]J. P. Hirt and J. Lothe, *Theory of Dislocations* (Wiley, New York, 1982), p. 862.
[14]E. R. Weber and H. Alexander, J. Phys. Colloq. **44**(C4), C4-319-C4-328 (1983).
[15]S. Pizzini, S. Binetti, A. Le Donne, A. Marzegalli, and J. Rabier, Appl. Phys. Lett. **88**, 211910 (2006).
[16]J. Rabier, Philos. Mag. A **93**, 162 (2013).
[17]A. N. Tereshchenko, E. A. Steinman, and J. Rabier, J. Phys.: Conf. Ser. **281**, 012020 (2011).
[18]N. Okuno and H. Saka, J. Mater. Sci. **48**, 115 (2013).
[19]L. Fedina, A. Gutakovskii, A. Aseev, J. Van Landuyt, and J. Vanhellemont, Philos. Mag. A **77**, 423 (1998).
[20]J. Hornstra, J. Phys. Chem. Solids **5**, 129 (1958).
[21]W. M. Lomer, London, Edinburgh, Dublin Philos. Mag. J. Sci. **42**, 1327–1331 (1951).
[22]A. S. Nandedkar and J. Narayan, Philos. Mag. A **61**, 873 (1990).
[23]A. Vila, A. Cornet, and J. R. Morante, Philos. Mag. A **71**, 85 (1995).
[24]L. Pizzagalli, J. Godet, and S. Brochard, Phys. Rev. Lett. **103**, 065505 (2009).
[25]M. J. Hytch, J.-L. Putaux, and J.-M. Penisson, Nat. Lett. **423**, 270 (2003).
[26]J. N. Stirman, P. A. Crozier, D. J. Smith, F. Phillipp, G. Brill, and S. Sivananthan, Appl. Phys. Lett. **84**, 2530 (2004).
[27]Y. Wang, P. Ruterana, S. Kret, J. Chen, S. El Kazzi, L. Desplanque, and X. Wallart, Appl. Phys. Lett. **100**, 262110 (2012).
[28]C. Zhao, S. Wen, Q. Hou, W. Qiu, Y. Xing, S. Su, and B. Cheng, J. Phys. Chem. Solids **90**, 87 (2016).
[29]C. Wen, Microsc. Microanal. **23**, 449 (2017).
[30]P. E. Batson and M. J. Lagos, Ultramicroscopy **180**, 34 (2017).
[31]V. V. Kveder, Yu. A. Osip'yan, and A. I. Shalynin, Zh. Eksp. Teor. Fiz. **83**, 699–714 (1982) [Sov. Phys. JETP **56**(2), 389–368 (1982)].
[32]K. Wessel and H. Alexander, Philos. Mag. **35**, 1523 (1977).
[33]A. T. Blumenau, M. I. Heggie, C. J. Fall, R. Jones, and T. Frauenheim, Phys. Rev. B **65**, 205205 (2002).
[34]W. Xie, J. Bang, and S. B. Zhang, Mater. Res. Lett. **2**(1), 51–56 (2014).
[35]A. Chuvilin and U. Kaizer, Ultramicroscopy **104**, 73–82 (2005).
[36]A. T. Blumenau, R. Jones, S. Öberg, P. R. Briddon, and T. Frauenheim, Phys. Rev. Lett. **87**, 187404 (2001).
[37]S. S. Kapur and T. Sinno, Phys. Rev. B **82**, 045205 (2010).
[38]A. Aseev, L. Fedina, D. Hoehl, and H. Barsch, *Clusters of Interstitial Atoms in Silicon and Germanium* (Academy Verlag, Berlin, 1994), p. 152.
[39]S. Takeda, M. Kahyama, and K. Ibe, Philos. Mag. A **70**, 287 (1994).
[40]L. I. Fedina and A. L. Aseev, Phys. Status Solidi A **95**(2), 517–529 (1986).
[41]L. I. Fedina, S. A. Song, A. L. Chuvilin, A. K. Gutakovskii, and A. V. Latyshev, Microsc. Microanal. **19**(S5), 38–42 (2013).
[42]L. I. Fedina, A. K. Gutakovskii, A. V. Latyshev, and A. L. Aseev, *Advances in Semiconductor Nanostructures* (Elsevier, 2017), Chap. 16, p. 527.
[43]S. Libertino, S. Coffa, and J. Benton, Phys. Rev. B **63**, 195206 (2001).
[44]L. Fedina, A. L. Aseev, S. G. Denisenko, and L. S. Smirnov, Mater. Sci. Forum **10–12**, 1123–1128 (1986).
[45]M. J. Hytch, E. Snoeck, and R. Kilaas, Ultramicroscopy **74**, 131 (1998).
[46]A. K. Gutakovskii, A. L. Chuvilin, and S. A. Song, Bull. Russ. Acad. Sci.: Phys. **71**, 1426 (2007).
[47]S. Binetti, S. Pizzini, E. Leoni, R. Somaschini, A. Castaldini, and A. Cavallini, J. Appl. Phys. **92**, 2437 (2002).